



# Application of chemical mechanical polishing process on titanium based implants



Z. Ozdemir<sup>a</sup>, A. Ozdemir<sup>b</sup>, G.B. Basim<sup>a,\*</sup>

<sup>a</sup> Ozyegin University, Faculty of Engineering, Mechanical Engineering Department, Nisantepi Mevki, Orman Sokak No: 26, Cekmekoy, Istanbul 34794, Turkey

<sup>b</sup> TUBITAK Gebze Campus, Genetic Engineering and Biotechnology Institute, P.O Box 21, Gebze, Kocaeli 41470, Turkey

## ARTICLE INFO

### Article history:

Received 14 January 2016

Received in revised form 26 April 2016

Accepted 1 June 2016

Available online 6 June 2016

### Keywords:

Implantable biomaterials

Surface structuring

Chemical mechanical polishing

Biocompatibility

## ABSTRACT

Modification of the implantable biomaterial surfaces is known to improve the biocompatibility of metallic implants. Particularly, treatments such as etching, sand-blasting or laser treatment are commonly studied to understand the impact of nano/micro roughness on cell attachment. Although, the currently utilized surface modification techniques are known to improve the amount of cell attachment, it is critical to control the level of attachment due to the fact that promotion of bioactivity is needed for prosthetic implants while the cardiac valves, which are also made of titanium, need demotion of cells attachment to be able to function. In this study, a new alternative is proposed to treat the implantable titanium surfaces by chemical mechanical polishing (CMP) technique. It is demonstrated that the application of CMP on the titanium surface helps in modifying the surface roughness of the implant in a controlled manner (inducing nano-scale smoothness or controlled nano/micro roughness). Simultaneously, it is observed that the application of CMP limits the bacteria growth by forming a protective thin surface oxide layer on titanium implants. It is further shown that there is an optimal level of surface roughness where the cell attachment reaches a maximum and the level of roughness is controllable through CMP.

© 2016 Elsevier B.V. All rights reserved.

## 1. Introduction

Biomaterials are commonly used to make implantable structures such as dental prostheses, orthopedic devices, cardiac pacemakers, stents and catheters [1]. The choice of an adequate implant material for a selected application is based on the bio-stability and bio-compatibility of the material once the required mechanical strength and durability is achieved. Commercially, pure titanium and its alloys (most commonly Ti-6Al-4V) are widely used as structural biomaterials due to their extraordinary properties such as high mechanical strength per unit volume in addition to their high corrosion resistance due to their stable passive oxide layer [1–4]. The native oxide layer of titanium that spontaneously forms in air is in nanometer scale (3–10 nm) and it is typically amorphous and stoichiometrically defective [5–6]. To be a protective oxide film, the formed TiO<sub>2</sub> layer has to be continuous, pore free and adhesive. Hence, although the native oxide film of titanium is known to be protective, additional oxidation treatments such as chemical etching [6], thermal treatment [7] and electrochemical anodization [8] of the titanium surface are practiced to grow an oxide layer by controlling the thickness, porosity, crystal structure of the oxide to enhance the wear characteristics as well as the bio-compatibility.

The nano-scale oxide layer of titanium has multiple functionalities in biomaterial implant. Spontaneously, when the titanium oxide film is continuous and pore free, it can also prevent the titanium ion dissolution once the implant is implanted applications. First of all, it is known to promote the biocompatibility of the titanium by enhancing cell attachment [9]. It also serves as an adhesion layer between the implant and the bone tissue (commonly simulated with hydroxyapatite-HA) particularly when an anatase crystalline structure is formed [10], which justifies the deposition of the TiO<sub>2</sub> layers on the bare titanium implants [7]. In addition, the formation of a protective oxide film of titanium helps shield the implant surface against corrosion by stopping the oxygen diffusion as shown by electrochemical analyses in detail [4]. As the implants are exposed to aggressive environments such as in body fluids (particularly in the acidic mouth environment when the dental implants are considered) the surface properties of this film becomes more important [4]. Consequently, it is favorable to promote the formation of the protective oxide layer of titanium during its processing for the implant applications.

In addition to the characteristics of the titanium oxide film, the surface topography of the titanium implants has also been studied intensively to analyze the effect of surface roughness on the biocompatibility. There are many processing techniques adopted to modify the implant material surface roughness and concurrently the chemical composition [11]. Gupta and coworkers classified the available surface

\* Corresponding author.

E-mail address: [Bahar.Basim@ozyegin.edu.tr](mailto:Bahar.Basim@ozyegin.edu.tr) (G.B. Basim).

modification techniques into four main groups including (i) the methods to increase surface roughness, (ii) chemical etching, (iii) various methods of coating and (iv) the surface chemical and chemical topography modifications [8]. Blasting is one of the most commonly practiced techniques to increase surface roughness in which particles of various diameters of mainly alumina ( $\text{Al}_2\text{O}_3$ ) and titania ( $\text{TiO}_2$ ) with particle size ranging from small, medium to large grit are used to blast the surfaces of the implant [12,13]. The obtained roughness depends on the particle size, time of blasting, pressure and distance from the source of particle to the implant surface. The created micro-scale roughness allows adhesion, proliferation and differentiation of bone cells (osteoblasts) yet the soft tissue cells (fibroblasts) adhere to the surface with difficulty and hence this method can limit soft tissue proliferation and increase bone formation. However, some particles are commonly left on the surface after blasting which may impair bone formation by a possible competitive action on calcium ions [14]. Chemical etching is another method in which the implant is dipped into an acidic environment and the surface structure changes as a function of acid type, concentration and exposure time. This method has also been observed to promote osteointegration and implemented following the sand blasting on the implant surfaces as well [15]. However, a yellowish, blurry looking film was observed to form on the implant surface after the etch operation [16]. Blasting method is also practiced by using only hydroxyapatite (HA) particles or biphasic calcium phosphate (BCP) particles. BCP is a mixture of the hydroxyapatite and beta-tricalcium phosphate. Implementation of an etch procedure is also common following the BCP treatment. The advantage of BCP is that the surface can be structured at micro-scale due to higher hardness of the BCP particles relative to pure HA. Moreover, even if the HA or BCP particles maybe left on the implant post blasting operation, they do not adversely impact biocompatibility since both of these minerals are known to have similar compositions to the bone tissue and they are commonly utilized to mimic the osteoblast attachment for implant studies [17]. Other than blasting and etching, application of coating on the implant surfaces with HA by using plasma spraying, laser ablation, pulsed laser deposition, sputtering or simply dip coating are also practiced [8]. While these methods help improve the cell attachment, they are also prone to delamination at the implant/coating interface, which may fail the healthy integration of the implant with the surrounding tissue [8,18]. Hydroxyapatite composites with zirconia and alumina were also shown to be good coating materials particularly for dental implants promoting the mechanical properties of the implants in addition to enhanced osteointegration [18]. Finally, the surface chemical and chemical topography modifications involve the treatment of the implant surface by the control of surface chemistry and attachment of proteins and cell adhesion molecules on the surfaces of the implant through electrical double layer interactions [8,19].

All the surface modification methods mentioned so far tend to form random surface structures on the implant surface ranging from nano to micro scale roughness. The isotropic nature of the surface structures result in equal probability of the cell attachment on the implant surface. To induce anisotropic surface structuring, more recently introduced alternative of implant surface structuring is the utilization of lasers [20–23]. The use of lasers allows the manufacturing of anisotropic surfaces which can help grow the cells in a specific direction. Furthermore, laser structuring can help in controlling cell attachment between the osteoblast which prefer micro-scale roughness and the fibroblast which is preferably better attached on the nano-rough surfaces [22,23]. It is also known that although micro-scale roughness has been studied intensively to promote cell attachment, the cellular events takes place on the nano-scale for cell-substrate interactions as the nano-metric cues have been shown to influence the cell activities [6,22,23]. Therefore, the scale of surface roughness from nano towards micro is critical to control bioactivity by selective promotion or demotion of the cell attachment.

In the present study we introduce chemical mechanical polishing (CMP) technique as an alternative to surface structuring of the biomedical implants [24]. CMP has initially been introduced for glass polishing and extended into the planarization of the interlayer metal connectors and dielectrics in microelectronics manufacturing [25]. In CMP process, the top film surface of the material is exposed to the chemicals in the polishing slurry which is made of submicron size particles and corrosives. This interaction forms a chemically altered top film that is removed by the mechanical action of the slurry abrasive particles. Therefore, it is a different method as compared to the mechanical polishing techniques used for implant surface finishing [26]. The chemically altered top films have to be a protective oxide to enable planarization by stopping chemical corrosion on the recessed metal surfaces while the elevated structures are polished [27]. Titanium CMP is performed in microelectronics to planarize Ti/TiN layers used as barriers to aluminum interconnect diffusion to the dielectric layers [28]. Furthermore, it has been shown by an earlier study that the application of CMP on Ti films has been very successful in terms of creating a titanium oxide film on the surface that might also help promote biocompatibility in addition to helping removal of the reacted and contaminated surface layers [16,29]. The comparison of the electrochemical etch to CMP application on titanium has shown that the titanium surfaces treated by CMP using colloidal silica slurries and an oxidizer concentration of 3 wt% were much clear and compositionally continuous than the yellowish and blurry titanium oxide layers formed by electrochemical etching. Furthermore, in this study CMP is synergistically utilized to induce nano-scale smoothness or nano/micro scale roughness on the bioimplant surface. Particularly, we focus on the dental implants to change the surface roughness in a control manner. Implementation of the CMP process on titanium bio-implants results in a synergy by (i) cleaning the implant surface from potentially contaminated surface layers by removing a nano-scale top layer during the process, (ii) simultaneously creating a non-porous and continuous nano-scale oxide film on the surface to limit any further contamination to minimize risk of infection and prevent corrosion and (iii) inducing controlled surface smoothness/roughness by designing the CMP process variables such as slurry particle size, solids loading as well as the oxidizer type and concentration.

In order to demonstrate the use of CMP on dental implants, both titanium plates and dental implants were processed. The CMP process was carried out by using alumina based slurries and  $\text{H}_2\text{O}_2$  as an oxidizer on commercially pure (cp) Ti samples with different polishing pads to modify surface topography. CMP characterization was performed by material removal rate, surface roughness by using atomic force microscopy (AFM) and wettability analysis (through contact angle measurements) in addition to the surface topography and elemental composition analyses on the treated surface by X-ray diffraction (XRD), energy dispersive X-ray spectroscopy (EDX) and X-ray photoelectron spectroscopy (XPS). Biological evaluations were performed by cytotoxicity evaluations in addition to bacterial and cell attachment tests and hydroxyapatite adhesion through wet deposition.

## 2. Materials and methods

### 2.1. Materials

The original titanium foil sample surface, which is considered as baseline in this experimental study, was annealed. Fig. 1a illustrates the optical micrograph of the anodized titanium plate surface (200X) as well as the SEM cross sectional image illustrating the thick and porous oxide layer with 30–40  $\mu\text{m}$  thickness. Fig. 1b shows the titanium based dental implant used to implement the optimized CMP conditions through hand polishing on a 3-D sample. The dental implants were provided by MODE Medical Company and they were only shaped by machining prior to their exposure to the CMP testing.

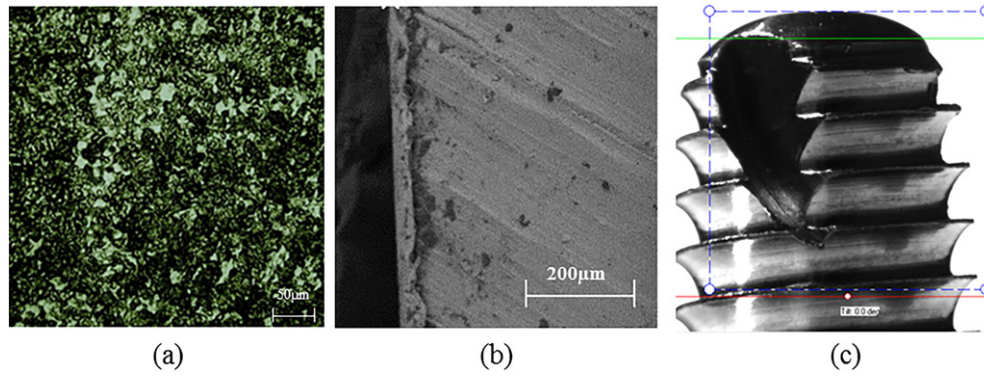


**Fig. 1.** Surface structures of (a) optical image of baseline anodized titanium plate sample ( $200\times$  magnification) and SEM x-section illustrating thick surface oxide, (b) baseline machine shaped dental implant sample with no additional surface treatment ( $4\times$  magnification).

## 2.2. Methods

### 2.2.1. Chemical mechanical polishing experiments

CMP experiments were conducted on a tabletop Tegrapol-31 polisher. Fig. 2a shows the 2-dimensional standard CMP set up as it is developed for the polishing and planarization of the 2-D structures. CMP slurries were prepared by using 5% weight alumina ( $\text{Al}_2\text{O}_3$ ) abrasives with 50 nm particle size at pH 4 using nitric acid. In order to provide stability, the suspensions were ultrasonicated long enough by repeated pH adjustment until the slurry was fully stabilized. CMP tests were conducted at 70 N downforce which is equivalent to a 7.88 psi pressure on the used sample size ( $14 \times 14$  mm). The titanium plates were polished by using a SubaIV subpad stacked under a polytex buff pad to smoothen the surface while protecting the macro-scale shape of the plates. This soft-pad configuration enables a gentle interaction between the pad and the implant surface providing local smoothening while maintaining the physical shape of the surface that is required for the screw pitch of the dental implants. In addition, two sizes of sand paper (silicon carbide 150C and P320) were used in place of the polishing pad to create the micro structures through CMP. Fig. 2b and c illustrate the CMP pads and the sample holder, respectively. In Fig. 2b, the picture with dark colored square surface structure belongs to the Polytex pad used as the prime pad and the lighter colored pad with the circular holes belongs to the Suba IV sub-pad. Hydrogen peroxide ( $\text{H}_2\text{O}_2$  – Sigma Aldrich, %34.5–36.5 purity) was utilized as an oxidizer in the CMP experiments except for the baseline sample which received no additional treatment. Furthermore, one of the samples was polished without an oxidizer to expose the underlying titanium metal in order to understand the effect of formation of an oxide layer during CMP on bio-compatibility. Samples ran with the polymeric CMP pads and

abrasive papers were polished for 2 min with 3 wt% oxidizer addition. Material removal rates were calculated through weighing the samples pre and post polish by Swiss Made ES125SM model precise scientific balance (five digits after the decimal point, 0.01 mg accuracy). All samples were cleaned in ultrasonic bath with pH 4-adjusted water for 5 min and dried with nitrogen gas before they were characterized. Same experimental procedure was implemented on the 3-D dental implant samples obtained from Mode Medical Limited by using a polymeric brush and flowing slurry on the samples as they were hand polished.

### 2.2.2. Surface characterization experiments

**2.2.2.1. Wettability characterization.** All the 2-D and 3-D samples were characterized for wettability through contact angle measurements with simulated body fluid (SBF) by using a KSV ATTENSION Theta Lite Optic Contact Angle Goniometer using the sessile drop method. Five drops were measured on each sample. The drop images were stored by a camera and an image analysis system calculated the contact angle ( $\theta$ ) from the shape of the drops.

**2.2.2.2. Surface topography and roughness characterization.** The surface topographies of the 2-D specimens were examined by Nanomagntics Atomic Force Microscope (AFM) using contact mode. Surface roughness values were recorded on  $10 \times 10 \mu\text{m}$  scan area and reported as an average of minimum three measurements taken on the samples. CMP generated metal oxide thin films are verified to be in nanometer scales (1–10 nm) and high energy beams of the Scanning Electron Microscopy (SEM) results in damage on these ultra-thin films, or require a coating to be applied (which changes the nature of the thin oxide layer). Therefore, AFM technique was preferred for characterization of the CMP

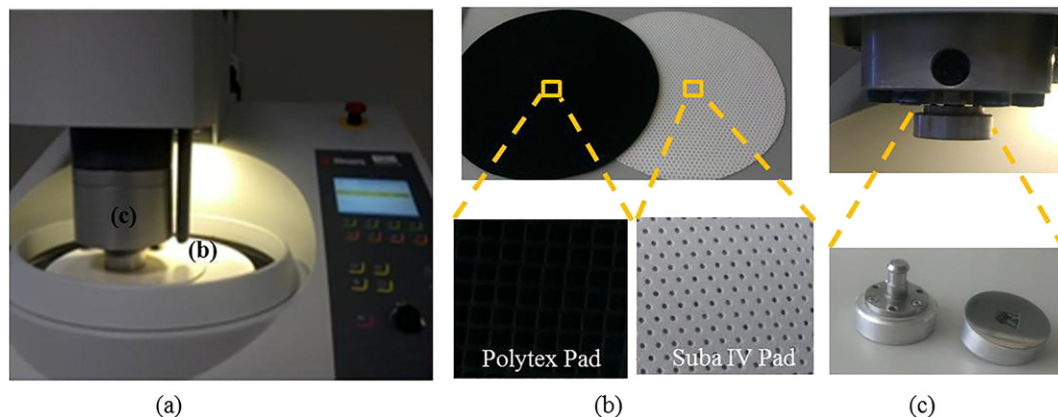


**Fig. 2.** CMP configuration for 2-D titanium plates (a) tabletop CMP tool (b) polytex and Suba IV polishing pads and (c) sample holder.

induced titanium surfaces (AFM does not require a coating application on the surface) [27,30]. SEM analyses were conducted to obtain the cross sectional analyses on the original titanium plate by JEOL JIB-4501SEM to analyze the thickness of the anodized titanium oxide layer. Furthermore, profilometry analyses were performed to measure the roughness values of the titanium plates at a larger scale by using a Mitutoyo SJ-400 profilometer. 4 mm lengths were scanned on the samples on three different locations and averaged for the average roughness (Ra) and average roughness depth (Rz) values.

**2.2.2.3. Surface crystallographic structure analyses.** In order to analyze the changes in the nature of the very top thin film that is modified by the chemical action of the CMP process, grazing angle GIXRD analyses were also conducted by using PANalytical, X'PERT Pro MPD model XRD analyzer. The XRD profiles were collected between 20–80° of 2θ angles with a step interval of 0.02° using grazing angles for the measurements.

**2.2.2.4. Surface chemical composition analyses.** The chemical nature of the titanium surfaces was also studied through X-ray photoelectron spectroscopy (XPS) and Energy Dispersive X-ray (EDX) analyses. PHOIBOS HAS 3500 150 R5e XPS [HW Type 30:14] tool was used to compare the electronic states of the Ti2p and O1s of the titanium plates pre and post CMP. Furthermore, EDX analyses were performed on a JEOL JIB-4501 MultiBeam Scanning Electron Microscope (SEM). The titanium peaks were investigated at 0.4 and 4.5 eV and oxygen peak was analyzed at the 0.525 eV as reference values [13].

### 2.2.3. Biostability and biocompatibility analyses

**2.2.3.1. Cytotoxicity analyses.** ISO 10993-5 cytotoxicity test procedure was adapted to evaluate the cell viability on the samples treated with and without CMP. L929 mice fibroblast cells were used to represent the mammalian system. Cells were counted and seeded onto the well plate at a concentration of 10<sup>4</sup> cells/plate. The titanium samples were kept in the solutions prepared as per the ISO 10993-5 procedures for 72 h and the solution extracts were added to the cell plates at 37 °C and retained for 24 h in a %5-CO<sub>2</sub> media. Cell viability was evaluated via WST-1 agent by colorimetric testing.

**2.2.3.2. Bacteria attachment evaluations.** Titanium plates were sterilized in an autoclave at 120 °C temperature for 20 min before the microbiological analysis. *Cronobacter sakazakii* (Gram-) bacteria was used as the species to evaluate the bacteria attachment. 100 μl of microorganisms from the nutrient broth microbial stock were spread on nutrient agar plates under sterile conditions. After the cultivation of bacteria, sterilized Ti samples were placed into each plate and incubated at 37 °C. The bacteria growth zone was observed over 1, 3 and 7 days and quantified by measuring the thickness of the colonies grown at the periphery of the plates through photographs taken on the samples (Fig. 3a).

**2.2.3.3. Cell growth analyses.** Titanium plates were cut into circular disks for the cell-growth evaluation to fit into well plate-18 and sterilized with UV radiation. L929 fibroblast cells were amplified in the laboratory for the proliferation on the samples. The cells were seeded directly on top of the Ti plates which were placed at the bottom of the wells. The nutrient medium was changed every 3 days to help keep the fibroblast cells alive. After 1, 3, and 5 days of incubation periods, the grown cells were washed off the titanium plates.

In order to test the cell attachment on the titanium plates, initially 7.8 g DMEM-F12 (Dulbecco's Modified Eagle Medium, D8900 Sigma) and 0.6 g NHCO<sub>3</sub> (dissolved in 450 ml ultra-pure water) was mixed to prepare a total 500 ml solution. The pH of the solution was adjusted to 7.3 with the addition of NaOH. 50 ml FBS (fetal bovine serum) was added afterwards to make a 10 wt% FBS concentrated solution. 5 ml of antibiotic Penicillin Streptomycin (100X) was added as the last component and the solution was mixed thoroughly and filtered as a final step. L929 fibroblast cells were grown in the prepared nutrient media inside the well plates in the presence of the prepared Ti samples. The excessive solution was removed from the well plates with vacuum and the plates were washed with phosphate buffer solution (PBS). The grown cells were separated from the plates by using Tripsin into the well plates. The cells were placed into the falcon tubes and centrifuged at room temperature at 1300 rpm. The settled cells were diluted to a 10<sup>4</sup> cells/cm<sup>2</sup> concentration and transferred on to the Thoma lamel for counting under the microscope as shown in Fig. 3b and c.

**2.2.3.4. Hydroxyapatite attachment analyses.** Hydroxyapatite (HA) is known to be mimicking the bone tissue as it is well studied in the literature and consequently it helps promote the osteoblast cell attachment as a coating on the implants [31–35]. In order to mimic the bone cell response, HA attachment was evaluated on the titanium implants by preparing a solution by using Ca and P routes namely the calcium nitrate (Ca(NO<sub>3</sub>)<sub>2</sub>) and diammonium hydrogen sulphate ((NH<sub>4</sub>)<sub>2</sub>HPO<sub>4</sub>) according to the reaction given in the following chemical Eq. (1) [31].



Before deposition, titanium samples were washed in distilled water in an ultrasonic bath. Deposition was carried out by dipping the titanium plates into the HA solutions for 72 h [32,33]. The HA growth was evaluated through weight differences pre and post the coating procedure. This evaluation is an indication of how well the osteoblast cells will attach to the CMP processed surface in addition to the plausibility of coating the implant surfaces with HA to further promote biocompatibility.

## 3. Results and discussion

The baseline titanium plates were anodized and hence had a porous oxide layer on the surface as it is seen in Fig. 1a. In order to understand the impact of the presence of oxide as well as the nature of the oxide

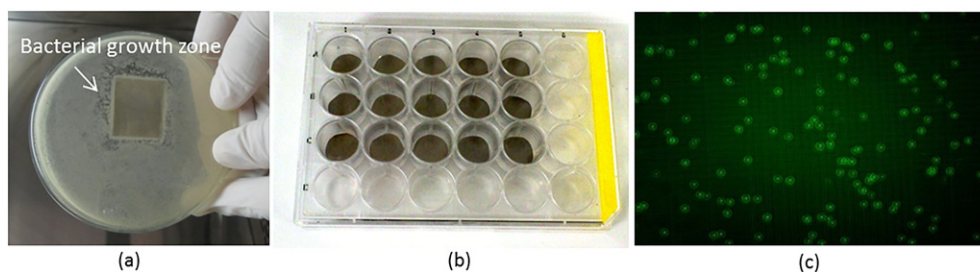


**Fig. 3.** Biological evaluation set-up for (a) bacterial growth analyses, (b) cell attachment test incubation well plates and (c) microscopic image of L929 cells on Thoma lamel used for counting fibroblast cells.

film on the titanium surface, a baseline sample was subjected to surface characterization and biological evaluations. In addition, another sample was prepared by implementing CMP treatment by using 3 wt% alumina nanoparticle containing slurry at pH 4 without addition of the H<sub>2</sub>O<sub>2</sub> oxidizer. This approach tunes the CMP process to function only mechanically and helps remove the surface oxide of the plates and expose the bare titanium without planarization due to the lack of chemical component. In addition, CMP was performed in the presence of oxidizer addition to the alumina slurries (3 wt% H<sub>2</sub>O<sub>2</sub>) in order to compare the titanium oxide films that forms through the CMP process to the baseline anodized oxide film in terms of bioactivity performance. In these preliminary CMP evaluations, a relatively soft polytex buff-pad was used on top of a SUBA IV subpad to provide smooth surface finish while protecting the topography of the surface such as the screw crests and roots of the dental implants. Following these treatments, two types of abrasive papers were used to induce micro-scale roughness to the titanium plates to evaluate the effect of surface nano-structuring on the material and biological responses by using the slurries in the presence of 3 wt% oxidizer. Consequently, five types of sample surfaces were prepared as (i) baseline, (ii) CMP without H<sub>2</sub>O<sub>2</sub> which exposes bare titanium surface, (iii) CMP treated in the presence of H<sub>2</sub>O<sub>2</sub>, (iv) CMP treated in the presence of oxidizer by using 45- $\mu$ m grid abrasive paper and (v) CMP treated in the presence of oxidizer by using 90- $\mu$ m grid abrasive paper. These five samples were evaluated for their CMP responses, surface characterization as well as the biological performances. Moreover, the 3-D dental implants were also exposed to the same set of treatments, as detailed in the materials and the methods section, and evaluated for their CMP responses and project corresponding biological performances.

### 3.1. CMP performance and wettability evaluations

Titanium plates treated with the five conditions as described above were initially characterized for the CMP material removal rate, wettability, and surface topography responses evaluated through surface roughness measurements. Table 1 summarizes the post CMP evaluations of the experiments conducted on the baseline and CMP treated titanium plates. It can be seen that the material removal rates of the samples polished on the polymeric pads were negligible. Particularly, the CMP test conducted without the addition of oxidizer resulted in only 0.007  $\mu$ m/min material removal rate. This result is expected since the material removal is driven by the continuous chemical attack on the surface by the oxidizer during the CMP operation. Consequently, when the oxidizer is added into the system, material removal rate of 0.5–0.9  $\mu$ m/min was obtained. On the other hand, polishing with the abrasive papers resulted in much higher removal rates due to the highly pronounced mechanical action provided by the fixed abrasive particles embedded into the polishing papers. Although, this very high level of material removal rates are typically not desired for the CMP applications, it must be noted here once again that the abrasive papers help modulate the surface roughness significantly to understand the effect of roughness on the bioimplant performance. Fig. 4a also illustrates the trend in the material removal rates of the samples treated with

various CMP conditions highlighting the much higher removal rates with the abrasive papers.

Fig. 4b summarizes the contact angle measurements taken with the simulated body fluid on the titanium plates representing the wettability of implant surface in the body environment. The high contact angle value obtained on the untreated baseline titanium sample can be attributed to the surface oxide formed by anodization which has a porous structure [34,35]. The trapped air in the porous titanium oxide is believed to increase the hydrophobicity of the surface. The CMP process performed without the oxidizer addition resulted in removal of the top oxide layer and exposed the titanium surface with a  $\sim 45^\circ$  contact angle measured, which is approximately half of the value measured on the baseline sample ( $85^\circ$ ). This observation confirms that the thick anodized oxide film was removed from the titanium surface during the polishing with water since the wettability response of the sample changed significantly. The decrease in the contact angle of the bare titanium surface can be attributed to the higher surface energy of the freshly exposed titanium atoms resulting in higher interaction with the water molecules that leads to higher surface wettability and hence a decrease in the contact angle value. For the following treatments where CMP was conducted in the presence of an oxidizer, the effect of surface roughness on the contact angle response started to dominate in parallel to the observations in the literature [21,22]. Fig. 5 shows the AFM micrographs and corresponding cross sectional analyses of the titanium plates treated by using five different experimental conditions. Here, it can be seen that the surfaces with a smoother surface finish, such as in the case of CMP application in the presence of the oxidizer (Fig. 5c), resulted in more wettability and hence a lower contact angle, and the surfaces with the induced micro-roughness (such as the samples polished with abrasive papers) resulted in a higher contact angle that can be attributed to the lowered wettability through the trapped air pockets within the grooves on the surface. One more important factor that can be observed by comparing the micrographs in Fig. 5 is that, the CMP of the surfaces by using the soft polytex pad helps smoothen the surfaces locally while protecting the macro scale topography. This effect can be seen when the cross-sectional profiles of the baseline sample (Fig. 5a) and the CMP treated sample (Fig. 5c) are compared.

Table 1 summarizes the surface roughness evaluations of the samples treated with the five experimental conditions by taking  $10 \times 10 \mu$ m surface scans and averaging the measurements on three samples. The original sample had a high root mean square (RMS) surface roughness ( $486 \pm 17$  nm) that can be attributed to the porous oxide layer formed by anodization. When the surface was buffed with CMP without the addition of the H<sub>2</sub>O<sub>2</sub>, the porous surface oxide was removed and the surface topography reduced to  $205 \pm 32$  nm. CMP process in the presence of the oxidizer at 3 wt% and using the polytex buff pad further reduced the surface roughness to  $128 \pm 41$  nm, achieving a smoother surface finish. When the abrasive papers were used, on the other hand, surface roughness increased as the grid size increased reaching up to  $517 \pm 88$  nm when the 90 mm grit size paper was used in place of the pad material.

The larger scale roughness measurements conducted with the profilometer were consistent with the AFM roughness values on the high surface roughness samples including the baseline sample and the

**Table 1**

Material removal rate, wettability and surface roughness responses of the titanium plate samples treated with five different experimental conditions.

Sample	CMP conditions		Material removal rate (nm/min)	Wettability contact angle ( $\theta$ )	RMS surface roughness (nm)	Profilometer surface roughness (nm)	
	Time (min)	Pad type				Ra	Rz
As is	–	–	–	$84.4 \pm 0.7$	$486 \pm 17$	$425 \pm 40$	$2660 \pm 50$
CMP without H <sub>2</sub> O <sub>2</sub>	2	Polytex pad	$7 \pm 2$	$45.6 \pm 1.2$	$205 \pm 32$	$410 \pm 20$	$2570 \pm 60$
CMP with 3 wt% H <sub>2</sub> O <sub>2</sub>	2	Polytex pad	$505 \pm 395$	$34.3 \pm 2.6$	$128 \pm 41$	$350 \pm 30$	$2470 \pm 120$
CMP with 3 wt% H <sub>2</sub> O <sub>2</sub>	2	Ab.P.(45 $\mu$ m)	$30,113 \pm 3039$	$54.2 \pm 0.2$	$423 \pm 56$	$350 \pm 50$	$2770 \pm 60$
CMP with 3 wt% H <sub>2</sub> O <sub>2</sub>	2	Ab.P.(90 $\mu$ m)	$37,260 \pm 3882$	$65.1 \pm 0.7$	$517 \pm 88$	$540 \pm 220$	$4170 \pm 1800$

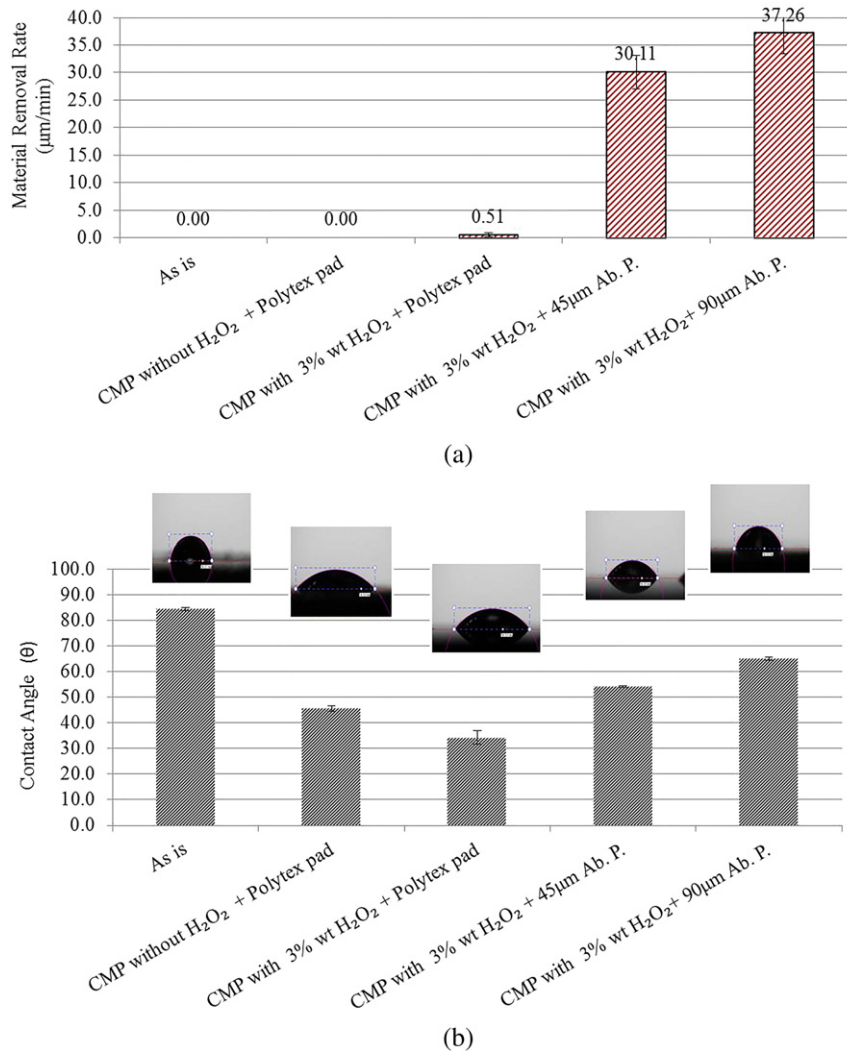


Fig. 4. Results of the (a) material removal rate and (b) surface wettability of the baseline and CMP treated Ti plates.

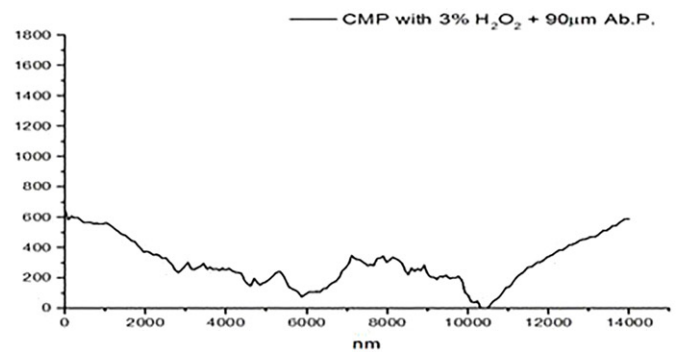
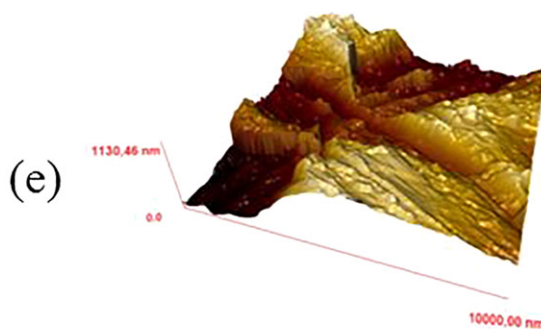
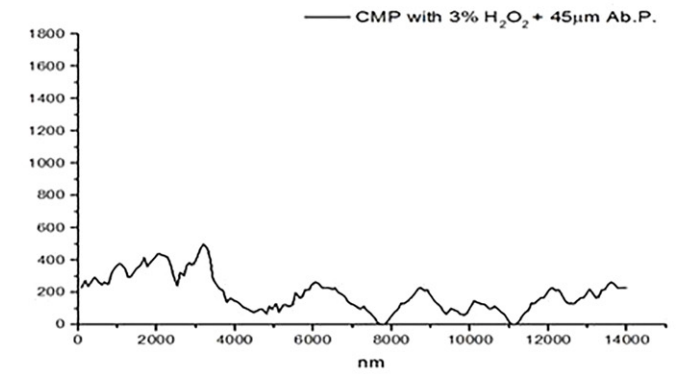
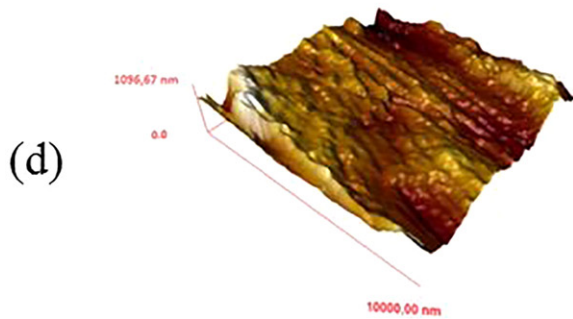
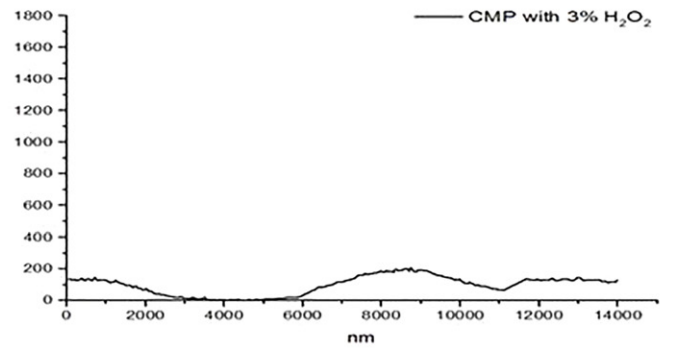
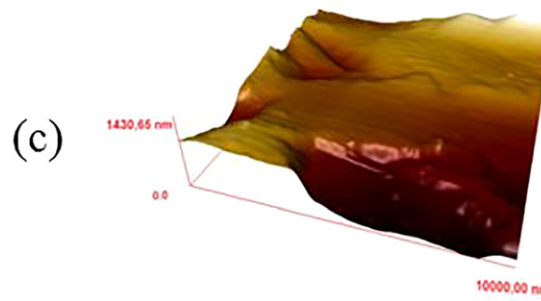
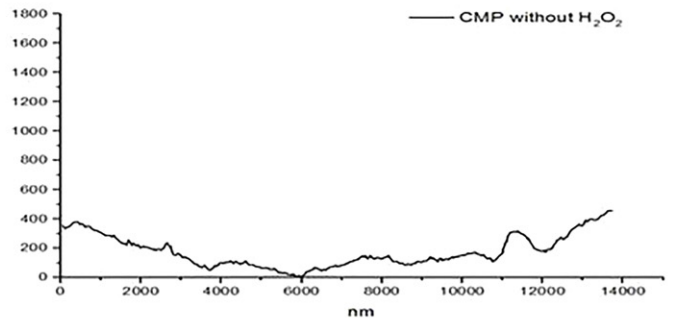
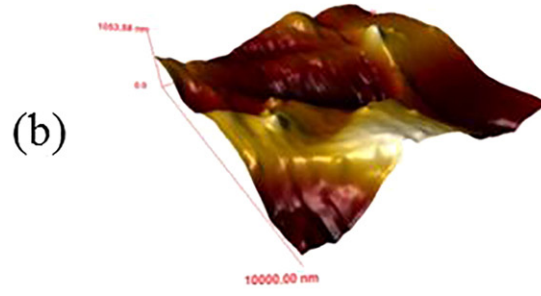
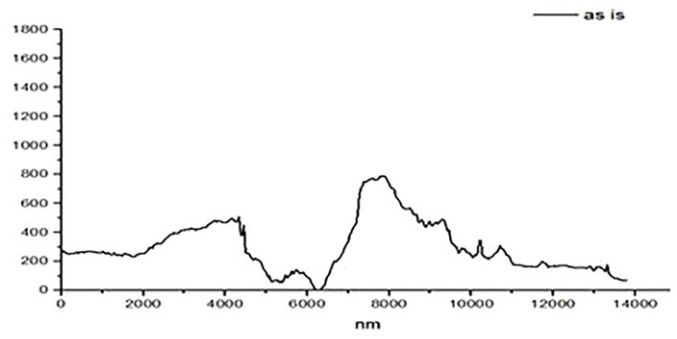
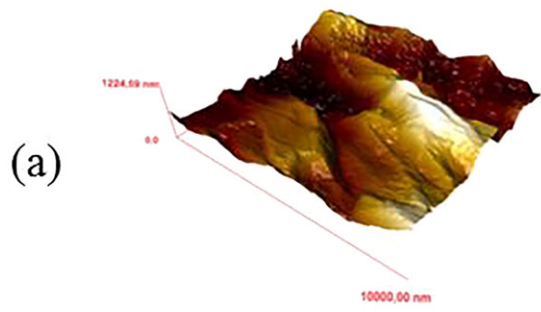
samples processed with CMP by using the abrasive papers. As it can be seen in Table 1, the baseline sample was measured as  $486 \pm 17$  nm by AFM and  $425 \pm 40$  nm (Ra) by the profilometer as an example. These values are statistically the same. However, for the samples processed by using the soft polishing pad in the absence and the presence of the oxidizer, AFM roughness values were reported as  $205 \pm 32$  nm and  $128 \pm 41$  nm, whereas profilometer roughness values were  $410 \pm 20$  nm and  $350 \pm 30$  nm, respectively. For these smoother samples, the local roughness measurements by AFM are giving smaller values as compared to the larger scale measurements by the profilometer and the results are statistically different. This finding is supporting the fact that the CMP treatment by the smooth pad usage is decreasing the surface roughness locally while still protecting the global curvature of the sample as desired. This result is also confirmed from the Rz measurement taken by the profilometer, in that, the average roughness depths are comparable for the relatively smoother samples ( $\sim 2400$ – $2800$  nm) yet the sample treated by using the largest grid abrasive paper has a Rz value of 4170 nm. These results further support the utilization of CMP as a method to control the surface roughness to enable the tuning for the needed biocompatibility.

### 3.2. Characterization of the surface oxide layer

The nature of the surface oxide forming on the titanium plates characterized for elemental composition as well as for the crystal structure. In order to determine the elemental composition, XPS analyses were performed. Furthermore, the changes in the crystallographic nature of the titanium surface in the absence and presence of the oxidizer in the CMP slurries were analyzed by XRD analyses to understand the protective nature of the surface oxide.

Fig. 6 shows the XPS spectrum of CMP treated titanium plates in the absence (only by using water in the CMP slurry) and presence of 3 wt% H<sub>2</sub>O<sub>2</sub> at the 2p orbital region of the titanium (Ti2p-region), and the 1s orbital region of the oxygen (O1s-region). This analysis was conducted to determine the changes in the intensities of the typical titanium and the oxygen peaks of the titanium plates as they are known to confirm the protective oxide formation on the surface [16]. A prominent Ti 2p<sub>3/2</sub> peak was observed at 459 eV region (Fig. 6a), which corresponds to the binding energy of Ti 2p<sub>3/2</sub> peak conformed to that of Ti in TiO<sub>2</sub>. Similarly, O 1s peak is positioned at the 530–535 eV region (Fig. 6b), which can be assigned to the three chemical components of oxygen namely (i) the lattice oxygen O<sup>2-</sup> (530.3 eV), (ii) the bridging and

Fig. 5. Post CMP treatment AFM micrographs and pre and post CMP cross sectional images of the titanium plates (a) as received baseline sample (b) post CMP without oxidizer (c) post CMP with 3% H<sub>2</sub>O<sub>2</sub> oxidizer (d) post CMP with 3% H<sub>2</sub>O<sub>2</sub> oxidizer with 45 µm grit abrasive paper and (e) post CMP with 3% H<sub>2</sub>O<sub>2</sub> oxidizer with 90 µm grit abrasive paper.



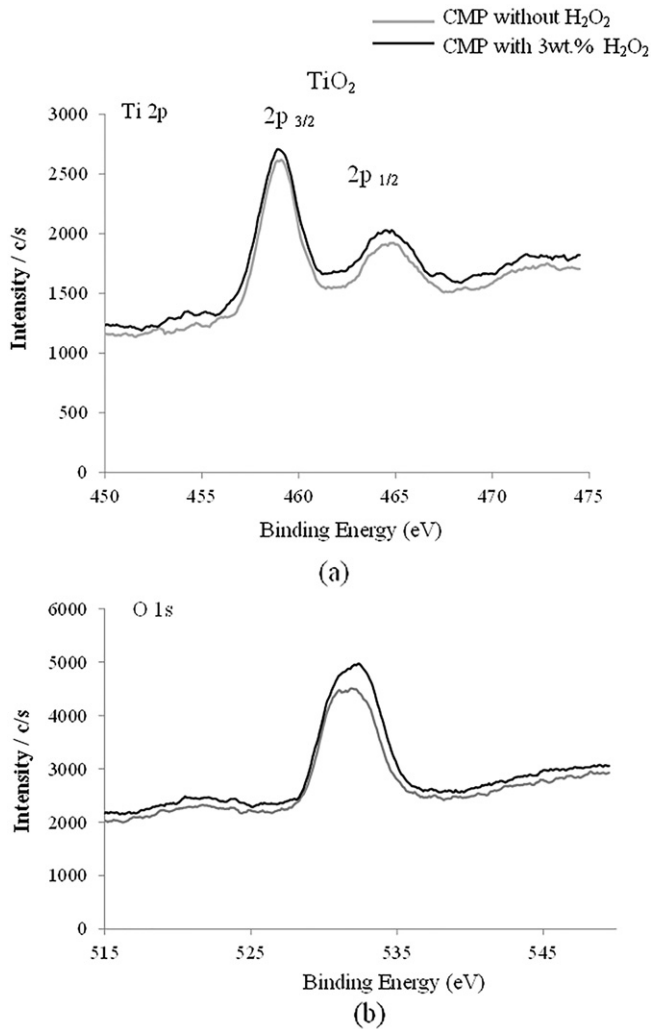


Fig. 6. XPS spectrum of CMP treated titanium plates in the absence (only by using water in the slurry) and presence of 3 wt% H<sub>2</sub>O<sub>2</sub> at (a) the Ti2p region and, (b) the O1s region.

**Table 2**  
Summary of EDX analyses on the titanium samples CMP treated with water versus 3% H<sub>2</sub>O<sub>2</sub>.

Sample	Element	Net	Nor. C (wt.%)	Atom C. (at.%)
CMP without H <sub>2</sub> O <sub>2</sub>	Titanium	19,954	93.95	84.49
	Oxygen	1145	5.35	14.39
CMP with 3 wt% H <sub>2</sub> O <sub>2</sub>	Titanium	17,997	88.01	72.94
	Oxygen	2045	9.33	23.15

terminal OH<sup>-</sup> (532.0 eV) and (iii) the adsorbed H<sub>2</sub>O peaks (533.2 eV) [17,18]. The samples polished by CMP in the presence of the oxidizer showed a higher intensity of the O1s peak relative to the samples polished by using only water in the slurry as seen in Fig. 6b. Yet, the Ti 2p<sub>3/2</sub> peaks of the titanium overlapped for both samples as seen in Fig. 6a. These results confirm the surface oxidation of the titanium plates when the oxidizer is used in the CMP slurry and indicate the formation of a protective oxide on the surface of the titanium [6,32]. In addition, Fig. 7 shows the EDX analyses performed on the CMP treated samples in the presence and absence of the oxidizer with soft pad. The results showed the surfaces of both samples are composed of titanium and oxygen. The net value of the oxygen was 5.30% on the sample treated with CMP by using only water, whereas the surface treated with CMP in the presence of oxidizer had a value of 9.02% as summarized in Table 2. As expected, the sample treated in the presence of oxidizer had a higher net value of oxygen and the corresponding titanium percentage was relatively lower in agreement with the XPS results.

In order to verify the protective nature of the CMP induced titanium oxide, the changes in the surface crystallographic nature of the titanium plates exposed to CMP treatment with and without the oxidizer addition was also studied by grazing angle X-ray diffraction analyses. This technique has the advantage of focusing on the thin film region of the sample surface and hence can give a precise comparison of the oxide thin film crystal structure forming during the CMP process. As it can be seen in Fig. 8, when hydrogen peroxide is added into the CMP slurries, the relative intensity of the Ti peak [33] reduced by 23% from 175 to 135, while the relative intensity of the titanium oxide peak (the anatase form of titania) [35] increased by 17% from 410 to 480. This data further agrees with the formation of a thin film of oxide layer on the surface of titanium plate when it is treated with the oxidizer in the slurries

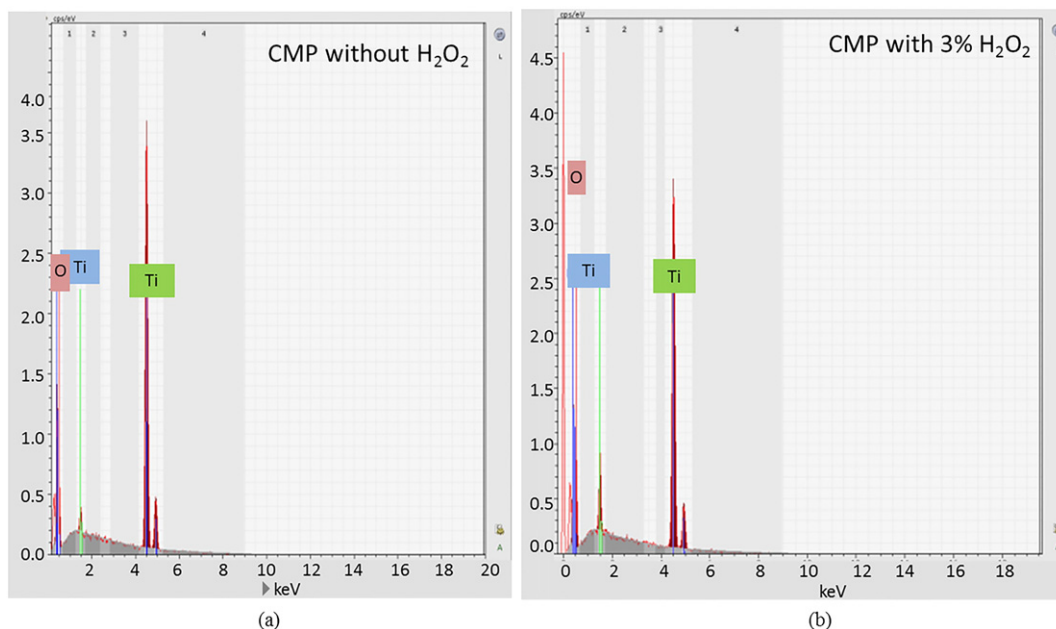


Fig. 7. EDX analyses on the titanium samples CMP treated with water only suspension versus with the addition of 3% H<sub>2</sub>O<sub>2</sub>.

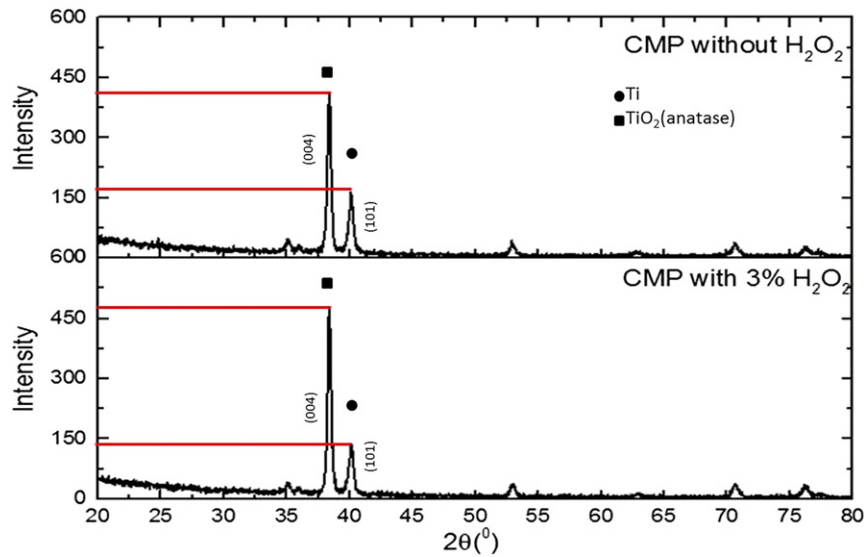


Fig. 8. XRD analyses on the titanium samples CMP treated with water only suspension versus with the addition of 3%  $H_2O_2$ .

during the CMP process. It can be concluded that a denser film of titania is formed when oxidizer is used as compared to the sample CMP treated by using only water. This is due to the faster conversion of the titanium atoms into titanium dioxide in the presence of the  $H_2O_2$  by oxidation reaction enhancing the protective nature of the oxide film on the implant material surface [32,37,38].

### 3.3. Bio-stability and bio-compatibility evaluations

#### 3.3.1. Cell viability analyses

In order to understand if there are any adverse effects of CMP treatment on the titanium implant material, the preliminary biological analyses were conducted to test the cell viability after the CMP application and the results were compared to the untreated sample. Fig. 9 shows the cytotoxicity test results conducted to evaluate the percent cell activity on the polished surfaces as compared to the baseline and the known positive and negative samples [39]. The results confirmed that the cell viability was not affected by the CMP process within the 72 h of the testing period. Furthermore, it is expected that the formation of the protective oxide films of titanium will further limit the titanium dissolution in longer term and hence improve the cell viability, which needs to be studied through in vivo evaluations.

#### 3.3.2. Bacteria growth analyses

Post CMP treatment biological evaluations were also performed through the bacteria growth analyses. Fig. 10 illustrates the growth zone thickness of the bacteria when the treated titanium plates were plated upside down in the petri dishes containing the nutrient fluid after 1, 3 and 7 days [40]. The baseline sample with a thick and porous oxide layer has shown an increase in the bacteria growth after the first day as the layer thickness increased from  $\sim 1.4$  mm to  $\sim 1.8$  mm. The same observation with a more pronounced effect has been noted on the titanium plate on which the oxide layer was removed through CMP application without using an oxidizer. The bacteria zone thickness increased to  $\sim 1.9$  mm from the first day value of 0.9 mm. This is believed to be due to the oxidation of the bare titanium surface in the nutrient solution. As the bacteria are known to grow on the oxide surfaces, the increase in the bacteria growth zone is potentially promoted when the oxide is formed [3,6]. This trend can also be explained by the increased hydrophobicity of the surface by the formation of the oxide, which promotes the biocompatibility [41]. When CMP is performed with 3 wt%  $H_2O_2$  addition, however, the results indicate that the increasing surface roughness promoted the bacteria zone thickness which can be attributed to the better adhesion of the bacteria on the rougher surface. Yet, all the samples were observed to retain an almost constant bacteria growth zone as a function of time after the CMP application. The consistency of

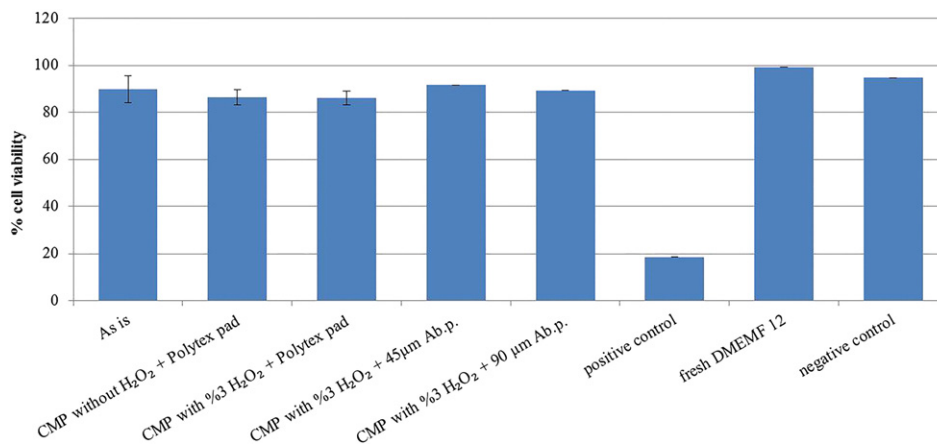
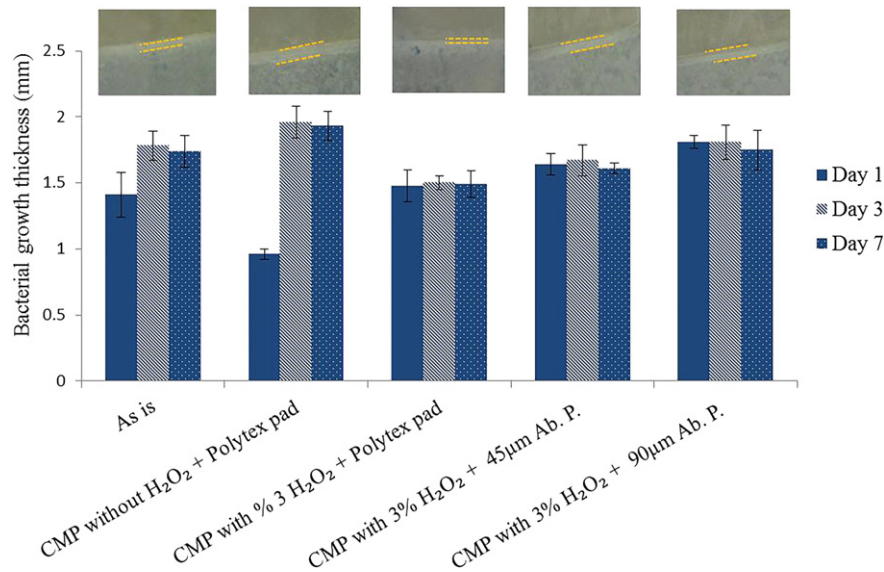


Fig. 9. Cell viability on the titanium samples treated with CMP as compared to the baseline and control samples to observation of the CMP process and chemical applied samples biocompatibility [35].



**Fig. 10.** Bacteria growth analyses on titanium plates quantified by thickness of the bacteria zone surrounding the titanium plates after 1, 3 and 7 days (reproduced with permission from Basim, Ozdemir and Karagoz, Copyright 2012 Cambridge University Press (USA) [36]).

the bacteria growth response of the CMP treated samples is believed to be due to the formation of a nano-scale protective oxide layer on the surface during the CMP process. Therefore, it is plausible that the control of surface roughness through CMP application can further be used to control the infection resistance.

### 3.3.3. Cell attachment analyses

The fibroblast type L929 cell attachment behavior was also evaluated on the titanium plates prepared by five different methods. Fig. 11 shows the change in the number of cells after 1, 3 and 5 days incubation in the well plates (after the fifth day the cells were observed to die due to lack of nutrient and hence the results were not reported). The cell growth increased on all the samples in consistency with the cell viability results. Yet, the growth rate showed a tendency to change by the surface roughness of the titanium plates. Samples surfaces which were CMP treated with the coarse abrasive papers and hence had a surface roughness of 400 nm and above (polished with 45 and 90 µm grit abrasive papers) have shown less amount of cell attachment. As it is schematically illustrated in Fig. 11 on the cross sectional images of the actual samples,

it can be suggested that the reason for this response is the sharp edges forming on the surface topography, which cause some of the cells to rupture as they try to approach and attach to the surface. Similarly, the baseline sample with a high RMS roughness value (~486 nm) also showed lower trend in cell attachment. On the other hand, the samples treated with CMP by using the polymeric polishing pads had smoother surface finish as it can be seen from their cross section images and the RMS surface roughness values reported in Table 1. Between these two surfaces, the best cell attachment was observed on the titanium plate which was CMP treated in the presence of the oxidizer. This plate had the smoothest surface finish (RMS surface roughness of ~120 nm) and a protective oxide film formed on its surface as shown in Figs. 6, 7 and 8. On the other hand, cell attachment was limited when the CMP was performed without an oxidizer and the pure titanium was exposed on the surface of the plate. This may be due to the dissolution of the  $Ti^{+4}$  ions in the absence of the protective oxide layer on the surface that limits the attachment of the cells. However, the standard deviations calculated based on three measurements do not show a statistically significant difference among the samples tested as observed by other

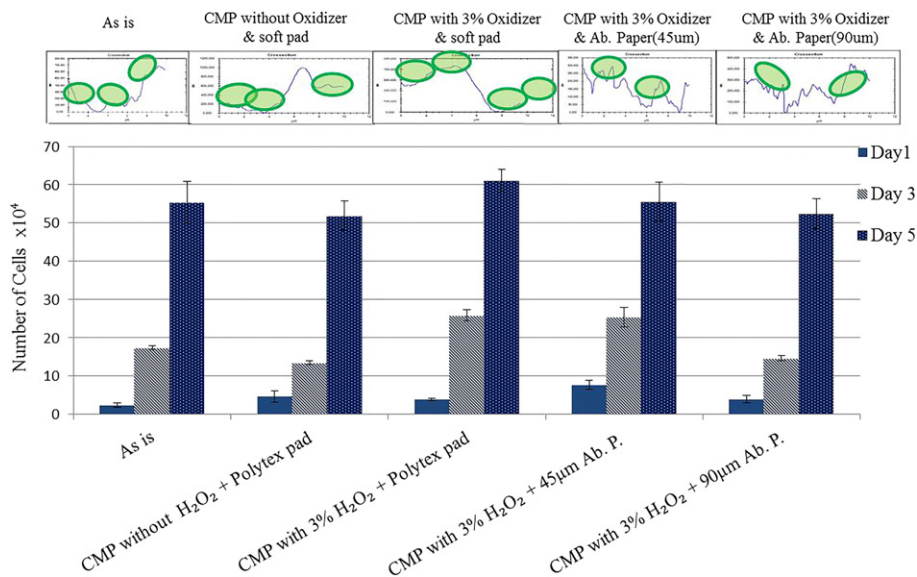


**Fig. 11.** L929 fibroblast cell attachment test results according to surface modification with CMP within a 5 days test period to observation proliferation distribution of cell.

researcher earlier [42]. Hence it can be stated that the CMP implementation increases the tendency of cell attachment when it is applied in the presence of oxidizers and using a soft pad promoting the smoothness. The sensitivity to the surface structuring is aligned with the earlier literature findings where the nano-scale structuring was observed to enhance the cell attachment [22,23].

### 3.3.4. Hydroxyapatite attachment analyses

Hydroxyapatite (HA) has been widely used as a coating material for dental implants due to its chemical composition similar to natural bone mineral and its capability to promote bone regeneration [19,42–44]. In this study, we have evaluated the HA attachment on the samples treated with CMP and once again compared the attachment performance to the baseline sample. Fig. 12a and b illustrate the HA attachment and the change in the RMS surface roughness values as a function of the HA coating, respectively. It can be seen that the attachment of HA increased with the increasing surface roughness. The smoothest surface obtained by the CMP in the presence of the oxidizer and the polytex pad resulted in the minimum amount of HA attachment which was 1.4 mg/72 h, while the surface with the highest roughness (polished with 90- $\mu\text{m}$  grid paper) resulted in 2.1 mg attachment/72 h. In addition, the post HA coating surface roughness values were higher when the original surface roughness was higher. The AFM micrographs given in Fig. 12b also clearly show the change in surface morphology with the HA coating. It is

interesting to note that although the pre-HA coating surface roughness of the baseline sample was similar to the roughness values obtained when the abrasive papers were used for CMP applications (45 and 90- $\mu\text{m}$  size sandpapers), the HA attachment was not similar on these samples. Fig. 13 demonstrates this difference much better when the cross sectional AFM micrographs of all the samples are compared pre and post HA deposition. Obviously, CMP induced surface roughness helped promote the HA attachment with a thicker layer deposited on the surface. This observation also supports the enhanced biocompatibility of the surfaces when CMP is applied since the HA attachment is known to promote the cell activity with increasing roughness on the HA coated surface reported to increase the osteoblast cell attachment in the earlier studies [42,43].

### 3.4. CMP application on 3-D dental implants

Fig. 14 summarizes the CMP performance of the 3-D dental implant samples which were obtained from MODE Medikal Inc. The same experimental procedure was followed on the 3-D dental implant samples by replacing the polymeric pad with a polymeric brush and hand polishing the samples all over their exposed surfaces with the alumina based polishing slurry. CMP performances were evaluated based on the material removal rates measured by the change in unit volume as a function of time and also measuring the wettability responses of the implant

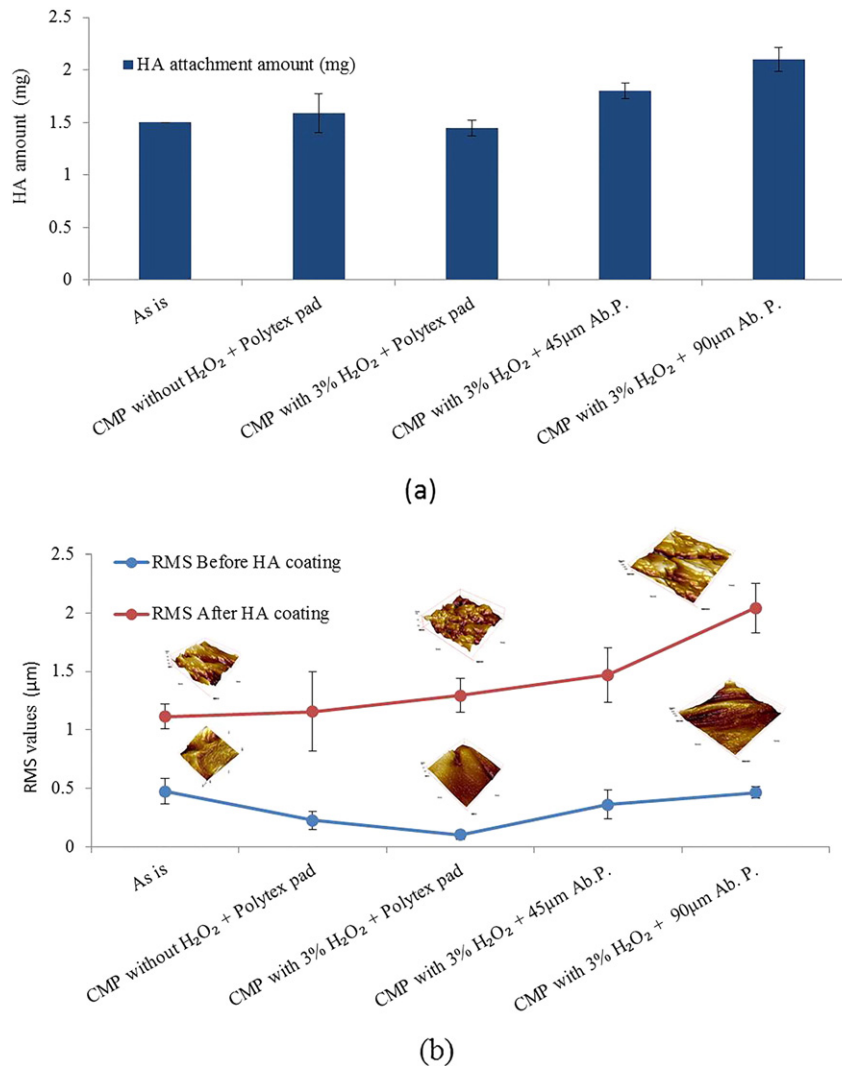
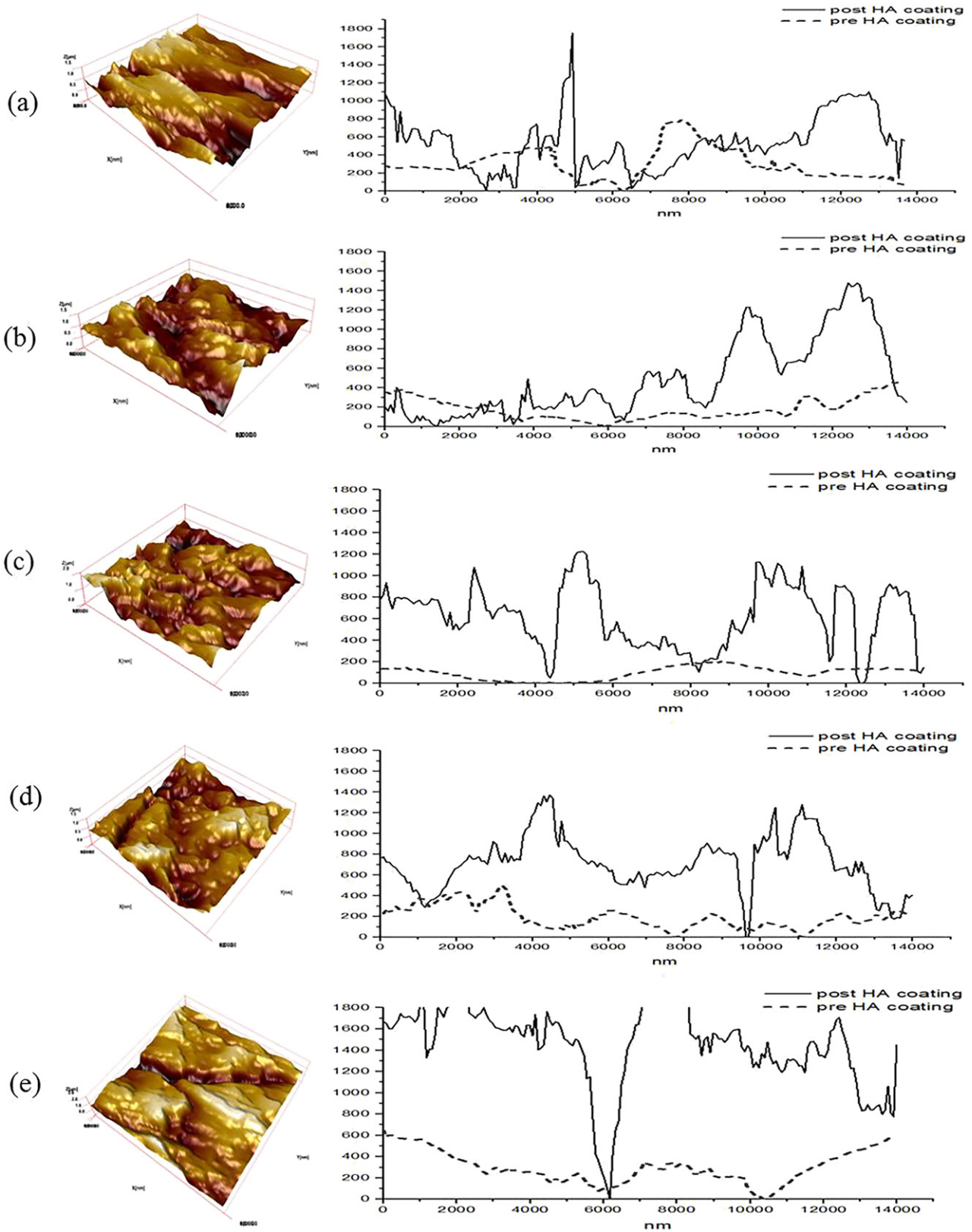


Fig. 12. HA attachment evaluation of the titanium samples (a) amount of HA attachment as a function of surface treatment and (b) measured RMS roughness values pre and post HA coating.



**Fig. 13.** Post HA coating AFM micrographs and pre and post cross sectional analyses of the titanium plates (a) as received baseline sample (b) post CMP without oxidizer (c) post CMP with 3% H<sub>2</sub>O<sub>2</sub> oxidizer (d) post CMP with 3% H<sub>2</sub>O<sub>2</sub> oxidizer with 45 μm grit abrasive paper and (e) post CMP with 3% H<sub>2</sub>O<sub>2</sub> oxidizer with 90 μm grit abrasive paper.

surfaces on a pre-selected region where the screw pitch is the same. It can be observed that both the material removal rate responses (Fig. 14a) and the wettability results maintained the same trend as

observed on the titanium plates. These results are encouraging in that the biological responses of the 3-D implants are expected to be similar to the 2-D equivalents.

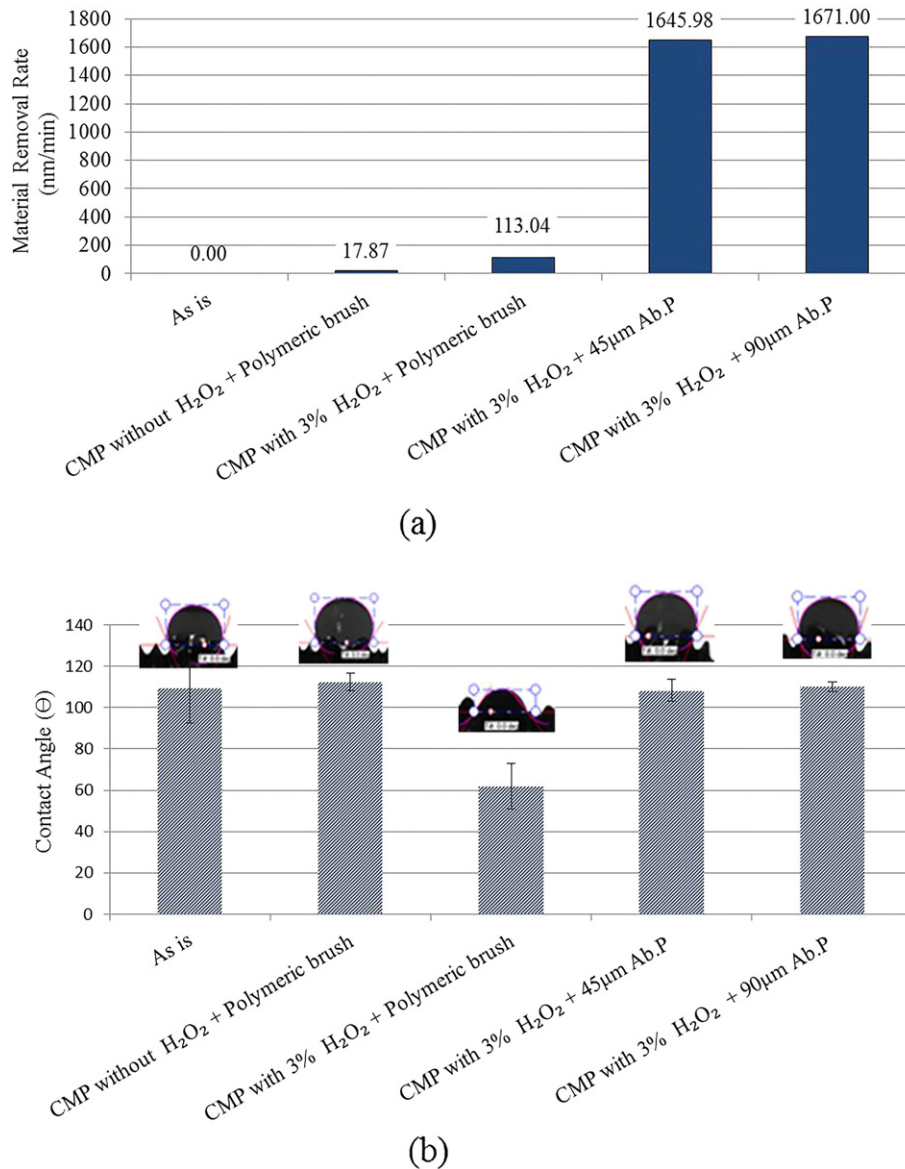


Fig. 14. CMP performance of the 3-D dental implants (a) material removal rate analyses and, (b) wettability responses post CMP treatment.

#### 4. Summary and conclusions

In this study we introduced CMP process as an alternative technique to engineer the titanium based implant surfaces to induce smoothness or controlled surface roughness while simultaneously forming a protective oxide layer. CMP technique was observed to help control the surface oxide thickness which has shown advantages in the bacteria growth analyses. The cell growth was observed to be affected more by the surface roughness and the cell attachment results have illustrated that there is an optimal roughness value where the cells are better adhering on the implant surface when their size match the surface structure better. Furthermore, HA attachment results also confirmed that the CMP treated surfaces tend to help the HA deposition more than an oxidized surface although the surface roughness values were comparable. The application of the CMP on the 3-D dental implant surfaces also resulted in similar CMP responses as compared to the 2-D plates confirming that the CMP application can help enhancing the surface properties of the titanium based implants.

In conclusion, CMP is a synergistic technique that can be implemented on the metallic implants by simultaneously forming a protective

oxide layer, limiting bacteria growth, controlling cell attachment as well as promoting the attachment of biocompatible coatings.

#### Acknowledgements

The authors would like to acknowledge the support from the European Union FP7 Marie Curie IRG (FP7-MC-IRG, NANO-PROX, Grant No: 256348) grant on the project entitled "Nano-Scale Protective Oxide Films for Semiconductor Applications & Beyond". Dr. Berrin Erdag and Mr. Koray Balcioglu at TUBITAK MAM-GEBI and Mr. Ozal Mutlu from Marmara University are also acknowledged for their contribution to the cell growth and bacteria zone growth analyses. The authors also would like to extend their appreciation to MODE Medikal for providing the dental implants.

#### References

- [1] D.R. Buddy, S.H. Allan, J.S. Frederick, E.L. Jack, *Biomaterials science: an introduction to materials in medicine*, second ed. Elsevier (2004).
- [2] J.R.S.M. Júnior, R.A. Nogueira, R.O. Araújo, Preparation and characterization of Ti-15Mo alloy used as biomaterial, *Mater. Res.* 14 (2011) 107–112.

- [3] C.N. Elias, J.H.C. Lima, R. Valiev, M.A. Meyers, Biomedical applications of titanium and its alloys, *JOM Biol. Mater. Sci.* 60 (2008) 46–49.
- [4] P. Schmutz, N.-C. Quach-Vu, I. Gerber, Metallic medical implants: electrochemical characterization of corrosion processes, *Electrochem. Soc. Interface* 1 (2008) 35–40.
- [5] E. Gemelli, N.H.A. Camargo, Oxidation kinetics of commercially pure titanium, *Matéria (Rio J.)* 12 (2007) 525–531.
- [6] F. Variola, Y.-H. Yi, L. Richert, J.D. Wuest, F. Rosei, A. Nanci, Tailoring the surface properties of Ti6Al4V by controlled chemical oxidation, *Biomaterials* 29 (2008) 1285–1298.
- [7] H. Guleryuz, H. Cimenoglu, Effect of thermal oxidation on corrosion and corrosion-wear behavior of a Ti-6Al-4V alloy, *Biomaterials* 25 (2004) 3325–3333.
- [8] Y.J. Cho, S.J. Heo, J.Y. Koak, S.K. Kim, S.J. Lee, J.H. Lee, Promotion of osseointegration of anodized titanium implants with a 1 $\alpha$ ,25-dihydroxyvitamin D3 submicron particle coating, *Int. J. Oral Maxillofac. Implants* 26 (2011) 1225–1232.
- [9] K. Shibata, A. Kamegai, Titanium in dentistry: biocompatibility of titanium, *Quintessence* (1988) 35–41.
- [10] I. Jouanny, S. Labdi, P. Aubert, C. Buscema, O. Maciejak, M.-H. Berger, V. Guipont, M. Jeandin, Structural and mechanical properties of titanium oxide thin films for biomedical application, *Thin Solid Films* 518 (2010) 3212–3217.
- [11] A. Gupta, M. Dhanraj, G. Sivagami, Implant surface modification: review of literature, *Internet J. Dent. Sci.* 7 (2009) 10.5580.
- [12] D.-H. Li, B.-L. Liu, J.-C. Zou, K.-W. Xu, Improvement of osseointegration of titanium dental implants by a modified sandblasting surface treatment: an in vivo interfacial biomechanics study, *Implant. Dent.* 8 (1999) 289–294.
- [13] H. Kim, S.-H. Choi, J.-J. Ryu, S.-Y. Koh, J.-H. Park, I.-S. Lee, The biocompatibility of SLA-treated titanium implants, *Biomed. Mater.* 3 (2008), <http://dx.doi.org/10.1088/1748-6041/3/2/025011>.
- [14] A. Wennerberg, T. Albrektsson, B. Andersson, Bone tissue response to commercially pure titanium implants blasted with fine and coarse particles of aluminium oxide, *Int. J. Oral Maxillofac. Implants* 11 (1996) 38–45.
- [15] R.G. Singh, A comparative analysis of sandblasted and acid etched and polished titanium surface on enhancement of osteogenic potential: an in vitro study, *J. Dent. Implant.* 2 (2012) 15–18.
- [16] S. Okawa, K. Watanabe, Chemical mechanical polishing of titanium with colloidal silica containing hydrogen peroxide-mirror polishing and surface properties, *Dent. Mater. J.* 28 (2009) 68–74.
- [17] M.-J. Lee, B.-O. Kim, S.-J. Yu, Clinical evaluation of biphasic calcium phosphate grafting material in the treatment of human periodontal intrabony defects, *J. Periodontol. Implant. Sci.* 42 (2012) 127–135.
- [18] I. Mobasherpour, M.S. Hashjin, S.S.T. Razavi, R.D. Kamachali, Effect of the addition ZrO<sub>2</sub>Al<sub>2</sub>O<sub>3</sub> on nanocrystalline hydroxyapatite bending strength and fracture toughness, *J. Ceram. Int.* 35 (2009) 1569–1574.
- [19] N. Lumbikanonda, R. Sammons, Bone cell attachment to dental implants of different surface characteristics, *Int. J. Oral Maxillofac. Implants* 16 (2001) 627–636.
- [20] A. Kurella, N.B. Dahotre, Review paper: surface modification for bioimplants: the role of laser surface engineering, *J. Biomater. Appl.* 20 (2005) 4–50.
- [21] N. Mirhosseini, P.L. Crouse, M.J.J. Schimidt, D. Garrod, Laser surface micro-texturing of Ti-6Al-4V substrates for improved cell integration, *Appl. Surf. Sci.* 253 (2007) 7738–7743.
- [22] H. Kenar, E. Akman, E. Kacar, A. Demir, H. Park, H. Abdul-Khalid, C. Aktas, E. Karaoz, Femtosecond laser treatment of 316L improves its surface nanoroughness and carbon content and promotes osseointegration: an in vitro evaluation, *Colloids Surf. B: Biointerfaces* 108 (2013) 305–312.
- [23] M. Oerringer, E. Akman, J. Lee, W. Metzgez, C.K. Akkan, E. Kacar, A. Demir, H. Abdul-Khalid, N. Pütz, G. Wennemuth, T. Pohlemann, M. Veith, C. Aktas, Reduced myofibroblast differentiation on femtosecond laser treated 316LS stainless steel, *Mater. Sci. Eng. C* 33 (2013) 901–908.
- [24] G.B. Basim, O. Bebek, S.O. Orhan, Z. Ozdemir, The Method of Processing Multidimensional Objects and Large and Curved Surfaces Using Chemical and Mechanical Nano Structure Method and Configuration of Robotic Arm Employed in Realizing This Method", PCT Patent Application, 2014 PCT/TR2014/000530.
- [25] G.B. Basim, Engineered Particulate Systems for Chemical Mechanical Planarization, Lambert Academic Publishing, 2011 ISBN 978-3-8433-6346-4.
- [26] C. Sittig, M. Textor, N.D. Spencer, Surface characterization of implant materials c.p. Ti, Ti-6Al-7Nb and Ti-6Al-4V with different pretreatments, *J. Mater. Sci. Mater. Med.* 10 (1999) 35–46.
- [27] F.B. Kaufman, D.B. Thomson, R.E. Broadie, M.A. Jaso, W.L. Guthrie, M.B. Pearson, M.B. Small, *J. Electrochem. Soc.* 138 (1991) 3460.
- [28] V.S. Chathapuram, T. Du, K.B. Sundaram, V. Desai, Role of oxidizer in the chemical mechanical planarization of the Ti/TiN barrier layer, *Microelectron. Eng.* 65 (2003) 478–488.
- [29] Y. Tanaka, E. Kobayashi, S. Hiroto, K. Asami, H. Imai, T. Hanawa, Calcium phosphate formation on titanium by low-voltage electrolytic treatments, *J. Mater. Sci. Mater. Med.* 18 (2007) 797–806.
- [30] A. Karagoz, V. Craciun, G.B. Basim, Characterization of nano-scale protective oxide films: application on metal chemical mechanical planarization, *ECS J. Solid State Sci. Technol.* 4 (2) (2015) 1–8.
- [31] M. dat-Shojai, M.-T. Khorasani, E. Dinpanah-Khoshdargi, A. Jamshidi, Synthesis methods for nanosized hydroxyapatite with diverse structures, *Acta Biomater.* 9 (2013) 7591–7621.
- [32] E. SaMcCafferty, J.P. Wightman, An X-ray photoelectron spectroscopy sputter profile study of the native air-formed oxide film on titanium, *Appl. Surf. Sci.* 143 (1999) 92–100.
- [33] Diffraction Data, JCPDS 44–1294.
- [34] J. Bico, U. Thiele, D. Quere, Wetting of textured surfaces, *Colloids Surf. A Physicochem. Eng. Asp.* 206 (2002) 41–46.
- [35] S.-H. Hsu, W.M. Sigmund, Artificial hairy surfaces with a nearly perfect hydrophobic response, *Langmuir* 26 (3) (2010) 1504–1506.
- [36] Diffraction Data, JCPDS 89–4921.
- [37] S. Ilango, G. Raghavan, M. Kamruddin, S. Bera, A.K. Tyagi, Surface morphology of annealed titanium/silicon bilayer in the presence of oxygen, *Appl. Phys. Lett.* 87 (2005) 101911 <http://dx.doi.org/10.1063/1.2042537>.
- [38] A.J. Nathananel, D. Mangalaraj, N. Ponpandian, Controlled growth and investigation on the morphology and mechanical properties of hydroxyapatite/titania nanocomposite thin films, *Compos. Sci. Technol.* 70 (2010) 1645–1651.
- [39] G.B. Basim, A. Karagoz, Z. Ozdemir, Characterization of chemically modified thin films for optimization of metal CMP applications, MRS Proceedings, 1560, MRS Spring Meeting, San Francisco, CA, 2013 <http://dx.doi.org/10.1557/opl.2013.876>.
- [40] G.B. Basim, Z. Ozdemir, A. Karagoz, Evaluation of infection resistance of biological implants through CMP based micro-patterning, MRS Proceedings, 1464, 2012 <http://dx.doi.org/10.1557/opl.2012.1469>.
- [41] A.S. Zuruzi, Y.H. Yeo, A.J. Monkowski, C.S. Ding, N.C. MacDonald, Superhydrophilicity on microstructured titanium surfaces via a superficial titania layer with interconnected nanoscale pores, *Nanotechnology* 24 (2013) 245304.
- [42] K. Li, K. Crosby, M. Sawicki, L.L. Shaw, Y. Wang, Effects of surface roughness of hydroxyapatite on cell attachment and proliferation, *J. Biotechnol. Biomaterials* 2 (2012).
- [43] S. Xu, Y. Xiaoyu, S. Yuan, T. Minhua, L. Jian, N. Aidi, L. Xing, Morphology improvement of sandblasted and acid-etched titanium surface and osteoblast attachment promotion by hydroxyapatite coating, *Rare Metal Mater. Eng.* 44 (2015) 67–72.
- [44] A.K. Nayak, Hydroxyapatite synthesis methodologies: an overview, *Int. J. ChemTech Res.* 2 (2010) 903–907.